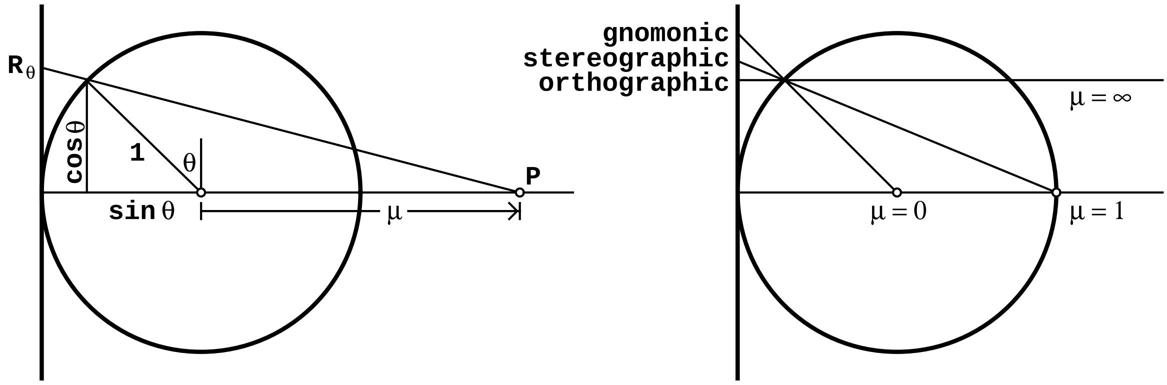

Fig. 4. (Left) geometry of the zenithal perspective projections, the point of projection at P is μ spherical radii from the centre of the sphere; (right) the three important special cases. This diagram is at 3:2 scale compared to the graticules of Figs. 8, 9 and 10.

hold unless (ϕ_0, θ_0) and hence (α_0, δ_0) does actually map to the reference point, $\phi_{\rm p}$ assumes its default value and the projection is scaled true at the reference point (some are not as discussed in Sec. 7.2). Figure 3 also illustrates the orientation of the native coordinate system with respect to the (x, y) coordinate system for the two main cases.

The requirement that (x, y) be measured in "degrees" begs clarification. Spherical projections are usually defined mathematically in terms of a scale factor, r_0, known as the "radius of the generating sphere". However, in this work r_0 is set explicitly to $180°/\pi$ in order to maintain backwards compatibility with the AIPS convention. This effectively sets the circumference of the generating sphere to 360° so that arc length is measured naturally in degrees (rather than radians as for a unit sphere). However, this true angular measure on the generating sphere becomes distored when the sphere is projected onto the plane of projection. So while the "degree" units of r_0 are notionally carried over by conventional dimensional analysis to the (x, y) they no longer represent a true angle except near the reference point (for most projections).

Cartographers, for example Kellaway (1946), think of spherical projections as being a projection of the surface of a sphere onto a plane, this being the *forward* direction; the deprojection from plane back to sphere is thus the *inverse* or *reverse* direction. However, this is at variance with common usage in FITS where the transformation from pixel coordinates to world coordinates is considered the forward direction. We take the cartographic view in this section as being the natural one and trust that any potential ambiguity may readily be resolved by context.

As stated in Sect. 1, (x, y) coordinates in the plane of projection, the native spherical coordinates, (ϕ, θ), celestial coordinates, (α, δ), and all other angles in this paper are measured in degrees. In the equations given below, the arguments to all trigonometric functions are in degrees and all inverse trigonometric functions return their result in degrees. Whenever a conversion between radians and degrees is required it is explicitly shown.

All of the graticules presented in this section have been drawn to the same scale in (x, y) coordinates in order to represent accurately the exaggeration and foreshortening found in some projections. It will also be apparent that since FITS image planes are rectangular and the boundaries of many projections are curved, there may sometimes be cases when the FITS image must contain pixels which are outside the boundary of the projection. These pixels should be correctly blanked and geometry routines should return a sensible error code to indicate that their celestial coordinates are undefined.

5.1. Zenithal (azimuthal) projections

Zenithal or *azimuthal* projections all map the sphere directly onto a plane. The native coordinate system is chosen to have the polar axis orthogonal to the plane of projection at the reference point as shown on the left side of Fig. 3. Meridians of native longitude are projected as uniformly spaced rays emanating from the reference point and the parallels of native latitude are mapped as concentric circles centred on the same point. Since all zenithal projections are constructed with the pole of the native coordinate system at the reference point, we set

$$(\phi_0, \theta_0)_{\rm zenithal} = (0, 90°)\,. \tag{11}$$

Zenithal projections are completely specified by defining the radius as a function of native latitude, R_θ. Rectangular Cartesian coordinates, (x, y), in the plane of projection as defined by Eq. (1), are then given by

$$x = R_\theta \sin\phi\,, \tag{12}$$
$$y = -R_\theta \cos\phi\,, \tag{13}$$

which may be inverted as

$$\phi = \arg(-y, x)\,, \tag{14}$$
$$R_\theta = \sqrt{x^2 + y^2}\,. \tag{15}$$

5.1.1. AZP: zenithal perspective

Zenithal (azimuthal) perspective projections are generated from a point and carried through the sphere to the

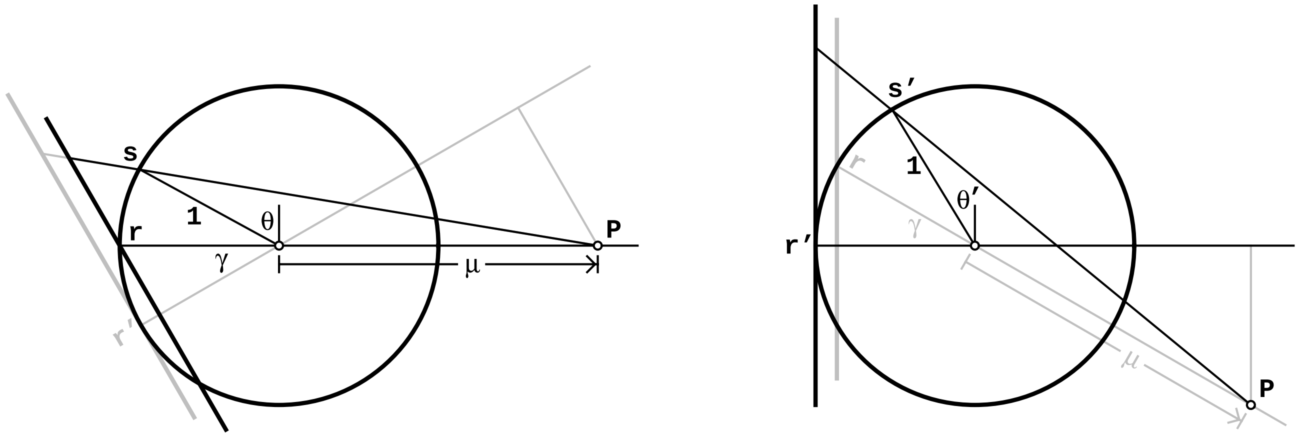

Fig. 5. Alternate geometries of slant zenithal perspective projections with $\mu = 2$ and $\gamma = 30°$: (left) tilted plane of projection (`AZP`), (right) displaced point of projection P (`SZP`). Grey lines in each diagram indicate the other point of view. They differ geometrically only by a scale factor, the effect of translating the plane of projection. Each projection has its native pole at the reference point, r and r', but these are geometrically different points. Thus the native latitudes θ and θ' of the geometrically equivalent points s and s' differ. Consequently the two sets of projection equations have a different form. This diagram is at 3:2 scale compared to the graticules of Figs. 6 and 7

plane of projection as illustrated in Fig. 4. We need consider only the case where the plane of projection is tangent to the sphere at its pole; the projection is simply rescaled if the plane intersects some other parallel of native latitude. If the source of the projection is at a distance μ from the centre of the sphere with μ increasing in the direction away from the plane of projection, then it is straightforward to show that

$$R_\theta = \frac{180°}{\pi} \frac{(\mu+1)\cos\theta}{\mu + \sin\theta}, \tag{16}$$

with $\mu \neq -1$ being the only restriction. When R_θ is given Eq. 16 has two solutions for θ, one for each side of the sphere. The following form of the inverse equation always gives the planeward solution for any μ

$$\theta = \arg(\rho, 1) - \sin^{-1}\left(\frac{\rho\mu}{\sqrt{\rho^2+1}}\right), \tag{17}$$

where

$$\rho = \frac{\pi}{180°} \frac{R_\theta}{\mu+1}. \tag{18}$$

For $|\mu| \neq 1$ the sphere is divided by a native parallel at latitude θ_x into two unequal segments which are projected in superposition

$$\theta_\mathrm{x} = \begin{cases} \sin^{-1}(-1/\mu) & \ldots |\mu| > 1 \\ \sin^{-1}(-\mu) & \ldots |\mu| < 1 \end{cases}. \tag{19}$$

For $|\mu| > 1$, the projection is bounded and both segments are projected in the correct orientation whereas for $|\mu| \leq 1$ it is unbounded and the anti-planewards segment is inverted.

A *near-sided* perspective projection may be obtained with $\mu < -1$. This correctly represents the image of a sphere, such as a planet, when viewed from a distance $|\mu|$ times the planetary radius. The coordinates of the reference point may be expressed in planetary longitude and latitude, (λ, β). Also, the signs of the relevant elements of the `CD`j_is matrix may be chosen so that longitude increases as appropriate for a sphere seen from the outside rather than from within. A first-order correction for planetary oblateness may also be applied through the `CD`j_is matrix.

It is particularly with regard to planetary mapping that we must generalize `AZP` to the case where the plane of projection is tilted with respect to the axis of the generating sphere as shown on the left side of Fig. 5. It can be shown (Sect. 7.6) that this geometry is appropriate for spacecraft imaging with non-zero look-angle, γ, being the angle between the camera's optical axis and the line to the centre of the planet.

Such *slant* zenithal perspective projections are not radially symmetric and their projection equations must be expressed directly in terms of x and y

$$x = R\sin\phi, \tag{20}$$

$$y = -R\sec\gamma\cos\phi, \tag{21}$$

where

$$R = \frac{180°}{\pi} \frac{(\mu+1)\cos\theta}{(\mu+\sin\theta) + \cos\theta\cos\phi\tan\gamma} \tag{22}$$

is a function of ϕ as well as θ. Equations 20 and 21 reduce to the non-slant case for $\gamma = 0$. The inverse equations are

$$\phi = \arg(-y\cos\gamma, x), \tag{23}$$

$$\theta = \begin{cases} \psi - \omega \\ \psi + \omega + 180° \end{cases}, \tag{24}$$

where

$$\psi = \arg(\rho, 1), \tag{25}$$

$$\omega = \sin^{-1}\left(\frac{\rho\mu}{\sqrt{\rho^2+1}}\right), \tag{26}$$

$$\rho = \frac{R}{\frac{180°}{\pi}(\mu+1) + y\sin\gamma}, \tag{27}$$

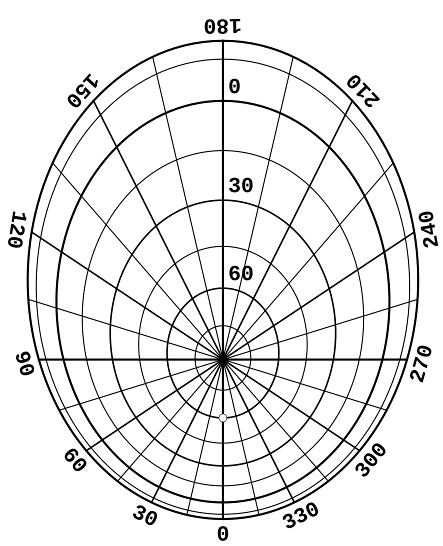

Fig. 6. Slant zenithal perspective (AZP) projection with $\mu = 2$ and $\gamma = 30°$ which corresponds to the left-hand side of Fig. 5. The reference point of the corresponding SZP projection is marked at $(\phi, \theta) = (0, 60°)$.

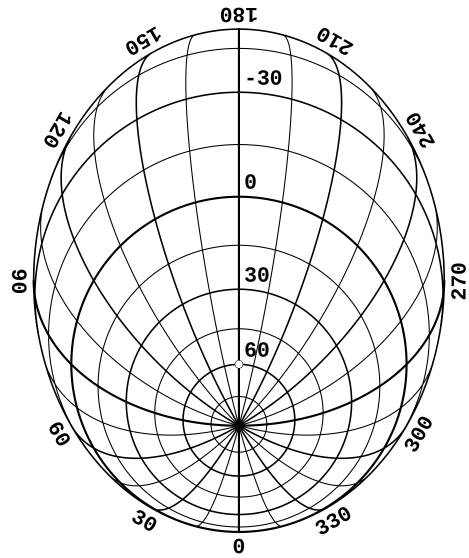

Fig. 7. Slant zenithal perspective (SZP) projection with $\mu = 2$ and $(\phi_c, \theta_c) = (180°, 60°)$ which corresponds to the right-hand side of Fig. 5. The reference point of the corresponding AZP projection is marked at $(\phi, \theta) = (180°, 60°)$.

$$R = \sqrt{x^2 + y^2 \cos^2 \gamma}\,. \tag{28}$$

For $|\mu| < 1$ only one of the solutions for θ will be valid, i.e. lie in the range $[-90°, 90°]$ after normalization. Otherwise there will be two valid solutions, the one closest to $90°$ should be chosen.

With $\gamma \neq 0$ the projection is not scaled true at the reference point and in fact the x and y scale is unequal there as can be seen in Fig. 6. This also shows the native meridians projected as rays emanating from the pole. For constant θ, each parallel of native latitude defines a cone with apex at the point of projection. This cone intersects the tilted plane of projection in a conic section. Eqs. 20 and 21 reduce to the parametric equations of an ellipse, parabola or hyperbola, the quantity

$$C = (\mu + \sin\theta)^2 - \tan^2\gamma \cos^2\theta \tag{29}$$

determines which:

$$\begin{aligned} C &> 0 \;\text{...ellipse,} \\ C &= 0 \;\text{...parabola,} \\ C &< 0 \;\text{...hyperbola.} \end{aligned} \tag{30}$$

If $|\mu \cos\gamma| \leq 1$ then the open conic sections are possible and $C = 0$ when

$$\theta = \pm\gamma - \sin^{-1}(\mu \cos\gamma)\,. \tag{31}$$

For $C > 0$ the eccentricity of the ellipse is a function of θ, as is the offset of its centre in y.

Definition of the perimeter of the projection is more complicated for the slant projection than the orthogonal case. As before, for $|\mu| > 1$ the sphere is divided into two unequal segments which are projected in superposition. The boundary between these two segments is what would be seen as the limb of the planet in spacecraft photography. It corresponds to native latitude

$$\theta_x = \sin^{-1}(-1/\mu)\,, \tag{32}$$

which is projected as an ellipse, parabola, or hyperbola for $|\mu \cos\gamma|$ greater than, equal to, or less than 1 respectively.

In general, for $|\mu \cos\gamma| > 1$, the projection is bounded, otherwise it is unbounded. However, the latitude of divergence is now a function of ϕ

$$\theta_\infty = \begin{cases} \psi - \omega \\ \psi + \omega + 180° \end{cases}, \tag{33}$$

where

$$\psi = -\tan^{-1}(\tan\gamma \cos\phi)\,, \tag{34}$$

$$\omega = \sin^{-1}\left(\frac{\mu}{\sqrt{1 + \tan^2\gamma \cos^2\phi}}\right). \tag{35}$$

Zero, one or both of the values of θ_∞ given by Eq. 33 may be valid, i.e. lie in the range $[-90°, 90°]$ after normalization.

The FITS keywords PVj_1s and PVj_2s, attached to *latitude* coordinate j, will be used to specify μ and γ respectively.

5.1.2. SZP: slant zenithal perspective

While the generalization of the AZP projection to tilted planes of projection is useful for certain applications it does have a number of drawbacks, in particular, unequal scaling at the reference point.

Figure 5 shows that moving the point of projection, **P**, off the axis of the generating sphere is equivalent, to within a scale factor, to tilting the plane of projection. However this approach has the advantage that the plane of projection remains tangent to the sphere and so the projection is conformal at the native pole as can be seen in Fig. 7. It is also quite straightforward to formulate the projection equations with **P** offset in x as well as y.

Although perhaps only of academic interest, this slant zenithal perspective (`SZP`) projection also handles the case which corresponds to $\gamma = 90°$ in `AZP`. `AZP` fails in this extreme since **P** falls in the plane of projection - effectively a scale factor of zero is applied to `AZP` over the corresponding `SZP` case. Perhaps the most important aspect of `SZP` is the application of its limiting case with $\mu = \infty$ in aperture synthesis radioastronomy as discussed in Sect. 5.1.5. One minor disadvantage is that the native meridians are projected as ellipses rather than straight lines.

If the Cartesian coordinates of **P** measured in units of the spherical radius are (x_p, y_p, z_p), then

$$x = \frac{180°}{\pi} \frac{z_p \cos\theta \sin\phi - x_p(1-\sin\theta)}{z_p - (1-\sin\theta)}, \quad (36)$$

$$y = -\frac{180°}{\pi} \frac{z_p \cos\theta \cos\phi + y_p(1-\sin\theta)}{z_p - (1-\sin\theta)}. \quad (37)$$

To invert these equations, compute θ first via

$$\theta = \sin^{-1}\left(\frac{-b \pm \sqrt{b^2 - ac}}{a}\right), \quad (38)$$

where

$$\begin{aligned} a &= X'^2 + Y'^2 + 1, && (39)\\ b &= X'(X - X') + Y'(Y - Y'), && (40)\\ c &= (X - X')^2 + (Y - Y')^2 - 1, && (41)\\ (X, Y) &= \frac{\pi}{180°}(x, y), && (42)\\ (X', Y') &= (X - x_p, Y - y_p)/z_p, . && (43) \end{aligned}$$

Choose θ closer to 90° if Eq. 38 has two valid solutions, then ϕ is given by

$$\phi = \arg\left(-(Y - Y'(1-\sin\theta)),\; X - X'(1-\sin\theta)\right). \quad (44)$$

The Cartesian coordinates of **P** are simply related to the parameters used in `AZP`. If μ is the distance of **P** from the centre of the sphere **O**, and the line through **P** and **O** intersects the sphere at (ϕ_c, θ_c) on the planewards side (point **r** in Fig. 5, right), then $\gamma = 90° - \theta_c$ and

$$\begin{aligned} x_p &= -\mu \cos\theta_c \sin\phi_c, && (45)\\ y_p &= \mu \cos\theta_c \cos\phi_c, && (46)\\ z_p &= \mu \sin\theta_c + 1, && (47) \end{aligned}$$

where μ is positive if **P** lies on the opposite side of **O** from **r** and negative otherwise. For a non-degenerate projection we require $z_p \neq 0$ and this is the only constraint on the projection parameters.

For $|\mu| > 1$ the sphere is divided into two unequal segments which are projected in superposition. The limb is defined by computing the native latitude θ_x as a function of ϕ

$$\theta_x = \begin{cases} \psi - \omega \\ \psi + \omega + 180 \end{cases}, \quad (48)$$

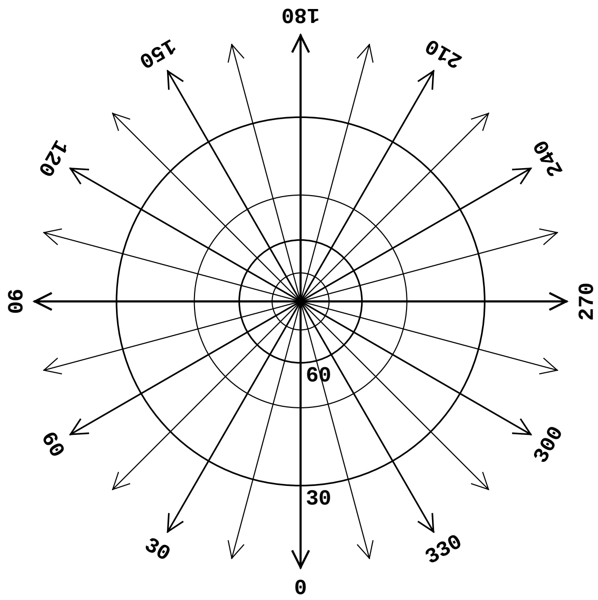

Fig. 8. Gnomonic (`TAN`) projection; diverges at $\theta = 0$.

where

$$\begin{aligned} \psi &= \arg(\rho, \sigma), && (49)\\ \omega &= \sin^{-1}\left(\frac{1}{\sqrt{\rho^2 + \sigma^2}}\right), && (50)\\ (\rho, \sigma) &= (z_p - 1,\; x_p \sin\phi - y_p \cos\phi), && (51)\\ &= (\mu \sin\theta_c,\; -\mu \cos\theta_c \cos(\phi - \phi_c)). && (52) \end{aligned}$$

Zero, one or both of the values of θ_x given by Eq. 48 may be valid, i.e. lie in the range $[-90°, 90°]$ after normalization. A second boundary constraint applies if $|1 - z_p| \leq 1$ in which case the projection diverges at native latitude

$$\theta_\infty = \sin^{-1}(1 - z_p). \quad (53)$$

The FITS keywords `PV`*j*`_1`*s*, `PV`*j*`_2`*s* and `PV`*j*`_3`*s*, attached to *latitude* coordinate *j*, will be used to specify μ, ϕ_c and θ_c respectively.

5.1.3. `TAN`: gnomonic

The zenithal perspective projection with $\mu = 0$, the gnomonic[5] is widely used in optical astronomy and was given its own code within the AIPS convention, namely `TAN`[6]. For $\mu = 0$ Eq. (16) reduces to

$$R_\theta = \frac{180°}{\pi} \cot\theta, \quad (54)$$

with inverse

[5] The gnomonic projection is the oldest known, dating to Thales of Miletus (ca. 624-547 B.C.). The stereographic and orthographic date to Hipparchus (ca. 190-after 126 B.C.).

[6] Referring to the dependence of R_θ on the angular separation between the tangent point and field point, i.e. the native *co*-latitude.

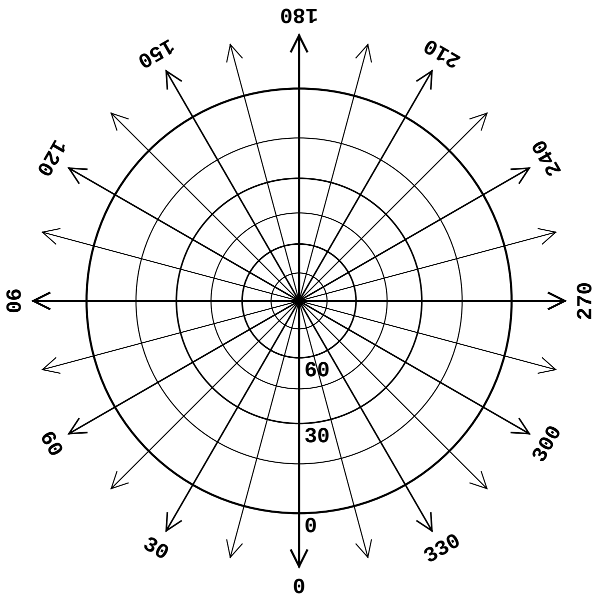

Fig. 9. Stereographic (STG) projection; diverges at $\theta = -90°$.

$$\theta = \tan^{-1}\left(\frac{180°}{\pi R_\theta}\right). \tag{55}$$

The gnomonic projection is illustrated in Fig. 8. Since the projection is from the centre of the sphere, all great circles are projected as straight lines. Thus, the shortest distance between two points on the sphere is represented as a straight line interval, which, however, is not uniformly divided. The gnomonic projection diverges at $\theta = 0$, but one may use a gnomonic projection onto the six faces of a cube to display the whole sky. See Sect. 5.6.1 for details.

5.1.4. STG: stereographic

The stereographic projection, the second important special case of the zenithal perspective projection defined by the AIPS convention, has $\mu = 1$, for which Eq. (16) becomes

$$R_\theta = \frac{180°}{\pi}\frac{2\cos\theta}{1+\sin\theta}, \tag{56}$$
$$= \frac{360°}{\pi}\tan\left(\frac{90°-\theta}{2}\right),$$

with inverse

$$\theta = 90° - 2\tan^{-1}\left(\frac{\pi R_\theta}{360°}\right). \tag{57}$$

As first realized by astronomer Edmond Halley (1656-1742), the stereographic projection illustrated in Fig. 9 is the conformal (orthomorphic) zenithal projection, everywhere satisfying the requirement for conformality of zenithal projections:

$$\frac{\partial R_\theta}{\partial\theta} = \frac{-\pi R_\theta}{180°\cos\theta}. \tag{58}$$

It also has the amazing property that it maps all circles on the sphere to circles in the plane of projection, although concentric circles on the sphere are not necessarily concentric in the plane of projection. This property made it the projection of choice for arab astronomers in constructing astrolabes.

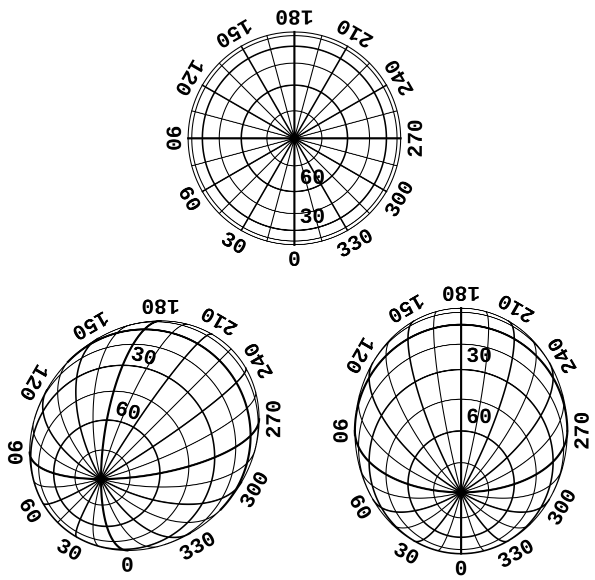

Fig. 10. Slant orthographic (SIN) projection: (top) the orthographic projection, $(\xi, \eta) = (0, 0)$, north and south sides begin to overlap at $\theta = 0$; (bottom left) $(\phi_c, \theta_c) = (225°, 60°)$, i.e. $(\xi, \eta) = (-1/\sqrt{6}, 1/\sqrt{6})$, (bottom right) projection appropriate for an east-west array observing at $\delta_0 = 60°$, $(\phi_c, \theta_c) = (180°, 60°)$, $(\xi, \eta) = (0, 1/\sqrt{3})$.

5.1.5. SIN: slant orthographic

The zenithal perspective projection with $\mu = \infty$, the orthographic, is illustrated in the upper portion of Fig. 10 (at consistent scale). It represents the visual appearance of a sphere, e.g. a planet, when seen from a great distance.

The orthographic projection is widely used in aperture synthesis radioastronomy and was given its own code within the AIPS convention, namely SIN[7]. Use of this projection code obviates the need to specify an infinite value as a parameter of AZP. In this case, Eq. (16) becomes

$$R_\theta = \frac{180°}{\pi}\cos\theta, \tag{59}$$

with inverse

$$\theta = \cos^{-1}\left(\frac{\pi}{180°}R_\theta\right). \tag{60}$$

In fact, use of the orthographic projection in radio interferometry is an approximation, applicable only for small field sizes. However, an exact solution exists where the interferometer baselines are co-planar. It reduces to what Greisen (1983) called the NCP projection for the particular case of an East-West interferometer as considered by Brouw (1971). The projection equations derived in Appendix C are

[7] Similar etymology to TAN.

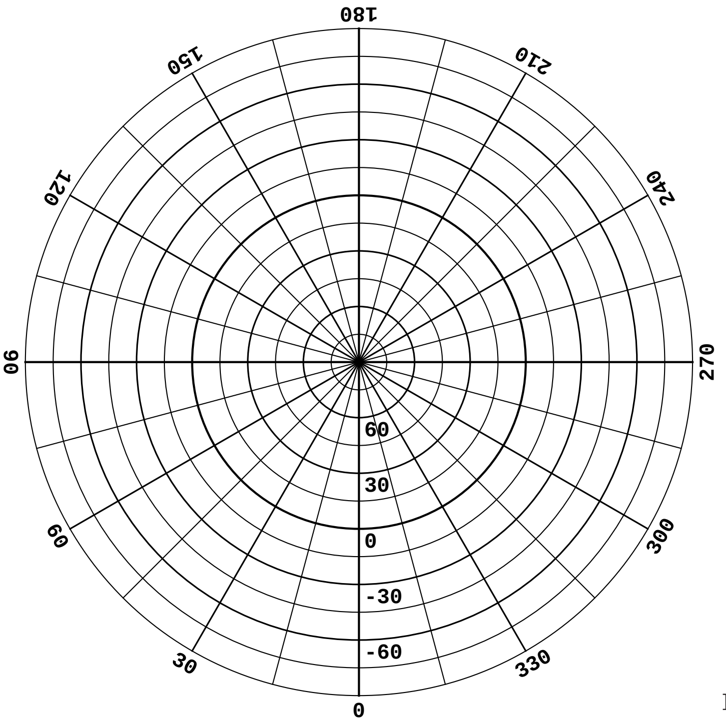

Fig. 11. Zenithal equidistant (ARC) projection; no limits.

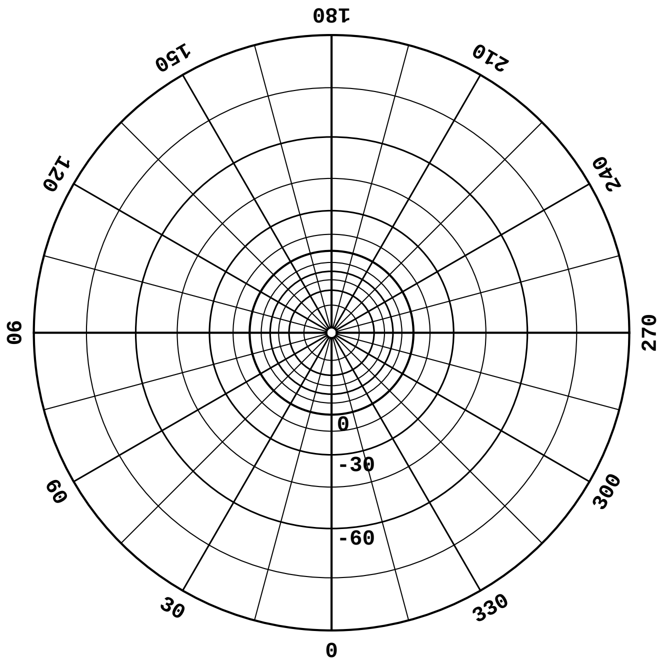

Fig. 12. Zenithal polynomial projection (ZPN) with parameters, 0.050, 0.975, -0.807, 0.337, -0.065, 0.010, 0.003, -0.001; limits depend upon the parameters.

$$x = \frac{180^\circ}{\pi} \left[\cos\theta \sin\phi + \xi\,(1 - \sin\theta)\right] , \quad (61)$$

$$y = -\frac{180^\circ}{\pi} \left[\cos\theta \cos\phi - \eta\,(1 - \sin\theta)\right] , \quad (62)$$

These are the equations of the "slant orthographic" projection, equivalent to Eqs. 36 and 37 of the SZP projection in the limit $\mu = \infty$, with

$$\xi = \cot\theta_c \sin\phi_c , \quad (63)$$

$$\eta = -\cot\theta_c \cos\phi_c . \quad (64)$$

It can be shown that the slant orthographic projection is equivalent to an orthographic projection centred at $(x, y) = \frac{180^\circ}{\pi}(\xi, \eta)$ which has been stretched in the ϕ_c direction by a factor of $\operatorname{cosec}\theta_c$. The projection equations may be inverted using Eqs. 38 and 44 except that Eq. 43 is replaced with

$$(X', Y') = (\xi, \eta) . \quad (65)$$

The outer boundary of the SIN projection is given by Eq. 48 in the limit $\mu = \infty$

$$\theta_x = -\tan^{-1}(\xi \sin\phi - \eta \cos\phi) . \quad (66)$$

Two example graticules are illustrated in the lower portion of Fig. 10. We here extend the original SIN projection of the AIPS convention to encompass the slant orthographic projection, with ξ and η given by keywords PVj_1s and PVj_2s, respectively, attached to *latitude* coordinate j.

5.1.6. ARC: zenithal equidistant

Some non-perspective zenithal projections are also of interest in astronomy. The zenithal equidistant projection first appeared in Greisen (1983) as ARC. It is widely used as the approximate projection of Schmidt telescopes. As illustrated in Fig. 11, the native meridians are uniformly divided to give equi-spaced parallels. Thus

$$R_\theta = 90^\circ - \theta , \quad (67)$$

which is trivially invertible. This projection was also known in antiquity.

5.1.7. ZPN: zenithal polynomial

The zenithal polynomial projection, ZPN, generalizes the ARC projection by adding polynomial terms up to a large degree in the zenith distance. We define it as

$$R_\theta = \frac{180^\circ}{\pi} \sum_{i=0}^{99} P_i \left(\frac{\pi}{180^\circ}(90^\circ - \theta)\right)^i . \quad (68)$$

Note the units implied by the $\frac{\pi}{180^\circ}$.

Since its inverse cannot be expressed analytically, ZPN should only be used when the geometry of the observations require it. In particular, it should never be used as an n^{th}-degree expansion of one of the standard zenithal projections.

If P_0 is non-zero the native pole is mapped to an open circle centred on the reference point as illustrated in Fig. 12. In other words, $(\phi_0, \theta_0) = (0, 90^\circ)$ is not at $(x, y) = (0, 0)$ which in fact lies outside the boundary of the projection. However, we do not dismiss $P_0 \neq 0$ as a